8 Microstrip Gas Chamber Development for HERAB and CMS

P. Robmann, S.Steiner, P.Truöl and T. Walter
in collaboration with the Universities of Heidelberg and Siegen

While there exists a reference design for the type of microstrip gas chamber (MSGC) which is to be used in the CMS central and forward/backward barrel tracker, the search for cheaper alternatives as well as designs with a more extended operation regime still continues actively. This was evident, when the forward/backward subgroup held one of their meeting in Zürich in November 1998.

The solution favored by most groups at the moment is a MSGC with a supplementary electron multiplier foil, termed GEM-MSGC (see last year's report [1]). This is also the type of chamber, which is being produced and installed for the inner tracker of the HERA-B experiment. We have designed masks for these chambers, controlled the quality of the substrates at produced industrially at IMT and started the design of the support structure for the chambers in the magnet.

In 1998 we also had two chamber test runs at PSI, one in July and another in October. A major part of the software for the data analysis of these runs was written in Zürich (in C^{++}), where we also analyse the data. The unfortunate conclusion from these runs, from the exposure of the chambers to an intense X-ray source in Heidelberg and to the HERA-B environment at DESY is, that a completely satisfactory solution for the inner tracker has not yet been found. Since the tests as well as the analysis are still in progress, only a few rather incomplete results can be given below.

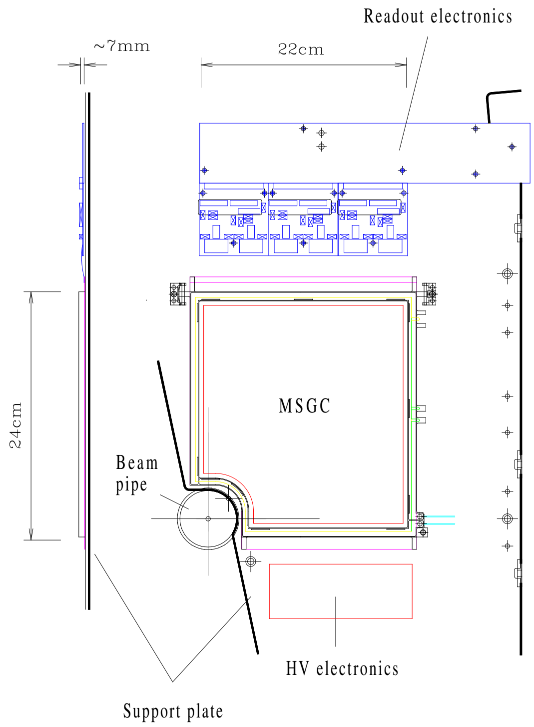

Figure 8.1: *HERA-B MSGC mounted on the support plate with the necessary readout and supply electronics.*

8.1 The GEM-MSGC detector for HERA-B

In Figure 8.1 the layout of a typical HERA-B MSGC is sketched. The chamber and the corresponding electronics, etc. are mounted on the support plate which is a compound of honey comb covered by a layer made out of carbon fibre on both sides.

The cover of the chamber consists of a 0.3 mm G10 plate (to ensure mechanical stability) and a 125 μm thick Kapton foil covered with 1 μm copper, which serves as the drift cathode. With a 3 mm drift gap the total chamber capacity is 200 pF. With a drift field in the range of 5.7 kV/cm we find a drift velocity of 52 mm/μs for an Argon/DME (50/50) mixture. The GEM foil, which is produced in the CERN workshop, is mounted below the drift gap. This 50 μm thick Kapton foil is covered with 7 μm copper on each side. The 55 μm diameter holes in the Kapton are staggered with a pitch of 140 μm, and are surrounded by a 90 μm diameter hole in the copper. An electronically stabilized voltage of about 390 V is applied between the upper and the lower surface of the GEM foil. Resistors of 2 MΩ on each side decouple the large cable capacity from the GEM capacity, which was measured as 30 nF. We expect a visible gas gain of about 20 to 30 in the GEM, determined from the size of the pulses seen at the output of the preamplifier-shaper. The charge produced in the GEM foil is transfered by an electrical field of about 5.2 kV/cm through the transfer gap of 2.8 mm to the MSGC wafer. The wafer substrate consists of 0.4 mm AF45 glass, which is coated with a diamond-like layer at the Frauenhofer Institut for Surface Engineering and Thin Films, Braunschweig, Germany. The coating has a thickness of about 0.08 μm and a typical surface resistance of 10^{14} Ω/square, about two orders of magnitude less than the bulk resistance of the glass. The electrode structure is produced with the lift-off technique by IMT in Greifensee, Switzerland. The production masks are manufactured from the layouts provided by us at IMT. The metallisation consists of a 0.5 μm thick, very soft gold layer on a 0.08 μm titanium which serves as the sticking layer to the coated substrate. For HERA-B three types of substrates are needed, types 1 and 2 have an active area of 220×240 mm^2 with 752 anodes (UZHHERA6, UZHHERA 5, substrate size 300×300 mm^2), and differ only in the size of the cutout near the beam pipe. The pitch is 300 μm, the anodes are 10 μm wide and the gap is 60 μm, resulting in 170 μm wide cathode strips. The active area of type 3 is 260×265 mm^2 with 756 anodes (UZHHERA7, substrate size 300×325 mm^2). Here the pitch is 350 μm and with the same anode and gap width as above the cathode strips are 220 μm wide. Sixteen cathodes are always connected together, which then form the 48 cathode groups. The layout for chamber type 2 was designed in 1997, for types 1 and 3 in 1998.

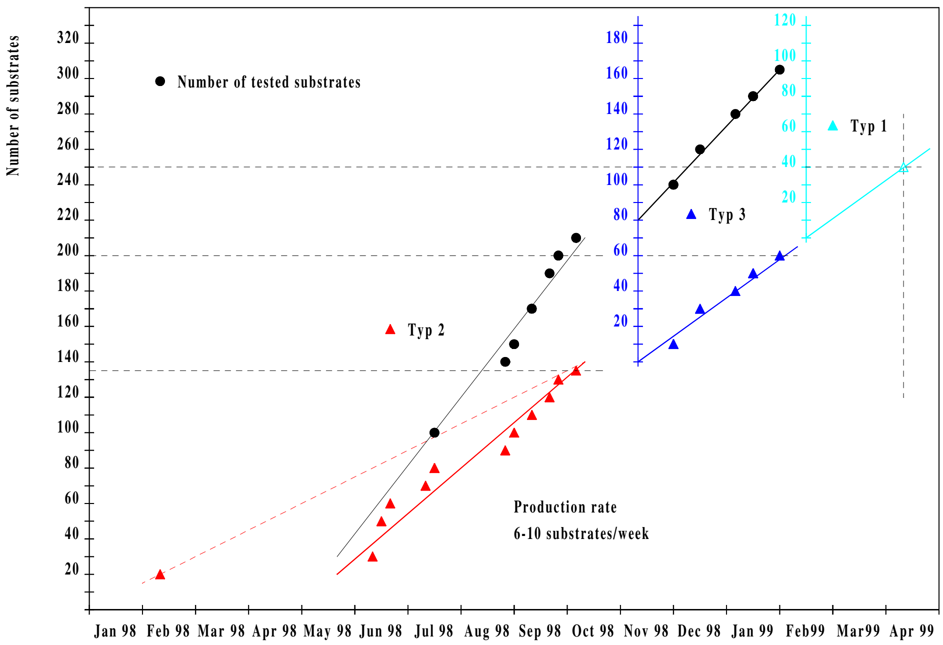

Figure 8.2: *Number of substrates produced at IMT (Greifensee) during the last year. The dots show the number of tested substrates.*

8.2 Substrate production and quality control at IMT

During the last year IMT produced about 200 substrates (see Figure 8.2), of which 135 type 2 and 58 type 3 are already accepted. The production of 40 type 1 substrates will finish by the end of April 1999. The quality of the substrate is controlled with the testing facility developed by us (see last year's report [1]). The setup is installed at IMT. This allows a fast feedback and guaranties a continous quality improvement. The dots in figure 8.2 show the number of tested substrates. Comparing this number with the number of accepted substrates shows a production yield of about 70%. An accepted detector substrate has to have less than 50 non-adjacent broken anodes and no shorts. Typically 15 or 2 % of the anodes are broken as Figure 8.3 indicates.

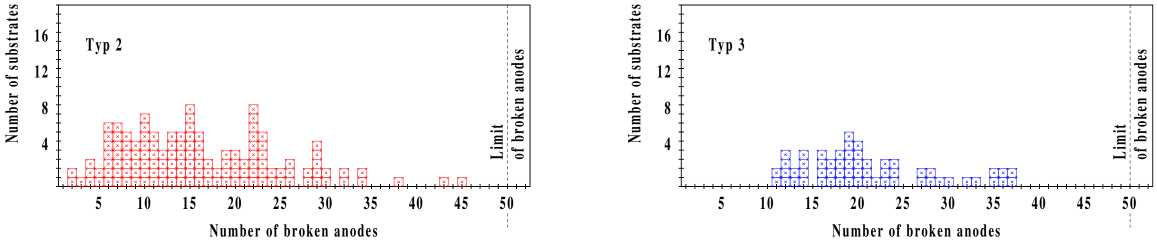

Figure 8.3: *Number of broken anodes for the accepted substrates of type 2 and type 3.*

8.3 MSGC tests at PSI

During the PSI test run in July for the first time a large GEM-MSGC with the fully pipelined readout system designed for the HERA-B experiment has been operated at high hadronic particle rates (see [2]). The system showed the expected performance with a relatively large gas amplification, which is not quantitavely understood yet. After subtracting correlated pickup signals and offset values channelwise the remaining noise is still somewhat higher than the expected thermal noise on the detector and input stage of the electronics. The correlation of the efficiency with additional occupancy due to noise shows that the operating conditions are realistic for a larger experiment, but the safety margin in signal amplitude is small (see Figure 8.4).

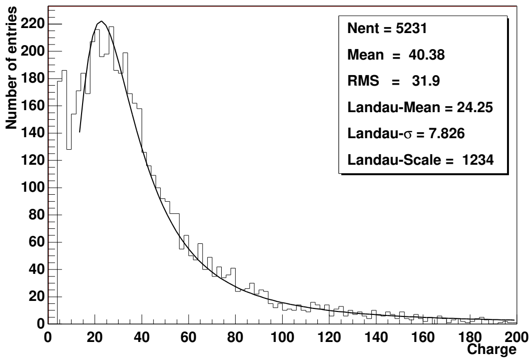

Figure 8.4: *Measured charge, the curve shows a fitted Landau distribution.*

In the October 1998 test run we operated a set of three detectors. This allows track reconstruction and the determination of efficiencies and spatial resolution. In Figure 8.5 the threshold dependence of the efficiency of the middle detector is plotted, when we are looking for tracks, which have a hit in the first and the last detector. In Figure 8.6 the residuals, i.e. the distance from the hit to the track, are plotted. The shift shows the missalignment of the setup of 120 μm.

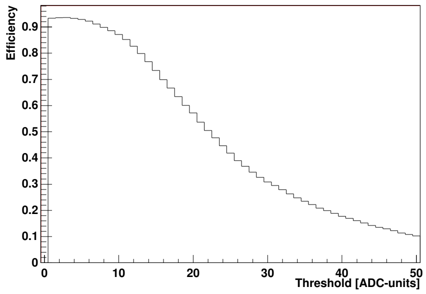

Figure 8.5: *Track finding efficiency depending on the threshold.*

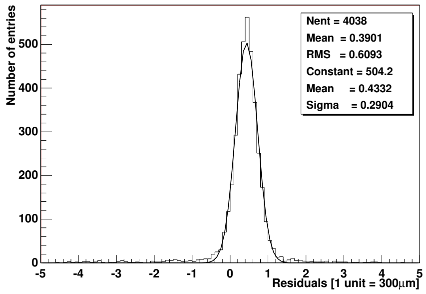

Figure 8.6: *Distribution of the residuals, the difference from the track to the measured hit.*

After irradiation with the high rate proton beam at PSI we observed ageing of the GEM-MSGC detectors. The gas ageing manifests itself by deposits on the irradiated anodes. The deposits (Carbon and/or C-H-moleculs) lead then to a reduction of the gas gain. Consequently the efficiency will also drop. Figure 8.7 shows a comparison of an anode from a new substrate and an anode from a substrate, which was irradiated at PSI. Laboratory ageing tests indicate, that the deposits originate from polluted materials used in the detectors.

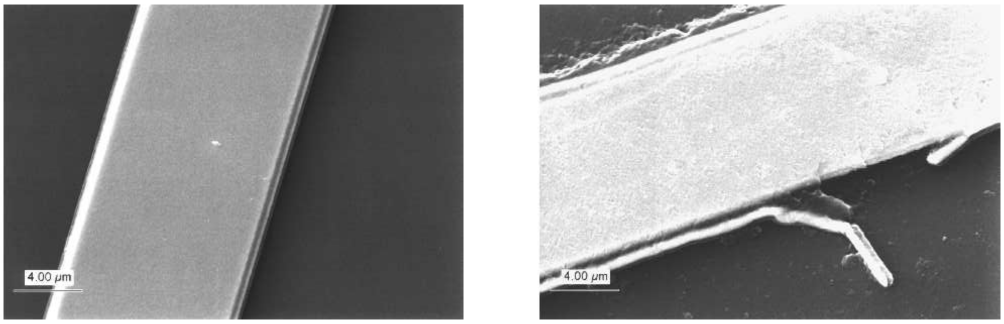

Figure 8.7: *REM picture of an Anode on a new substrate (left) and picture of an anode, irradiated during the test at PSI in October 1998 (right).*

8.4 Status of the HERA-B experiment

The HERA-B experiment is part of the worldwide effort to understand the origin of the baryon-antibaryon asymmetry in the universe related to the small observed CP-violation in the neutral kaon system. The electroweak standard model, in which the physical states are related to the weak eigenstates through the quark mixing matrix incorporates CP-violation. The observed charge asymmetry in K_L^0 decay as well as the coexistence of K_L^0 decays into two and three pions are both consistent with the electroweak standard model, but can not yet taken as proof, that nature has taken this path. The standard model predicts larger asymmetries in the decays of neutral B-mesons, which is why most of the experimental effort is directed to this system. Three avenues are taken, using hadron colliders, using electron-positron colliders and directing the highest energy proton beams available onto fixed targets. The experiments BaBar and Belle at an high-intensity e^+e^- storage ring (SLAC B-factory) operating at a center of mass energy of 10.5 GeV and producing $B_d\overline{B}_d$ pairs are starting this year. The 1 TeV $\overline{p}p$ collider at Fermilab with its two experiments D0 and CDF resumes operation next year with increased luminosity. It is with these four experiments, which the HERA-B experiment competes.

Effects to further scrutinize the information from the K^0 system continue. The combined results from precision experiments at CERN and Fermilab comparing the charged and neutral two pion decays of the K_L^0 and measuring the parameter ϵ'/ϵ [3] indicate a direct CP-violation in the decay, not only induced through quark mixing. Future experiments at Brookhaven and Fermilab propose to measure the extremely rare decay $K_L^0 \to \pi^0\nu\overline{\nu}$.

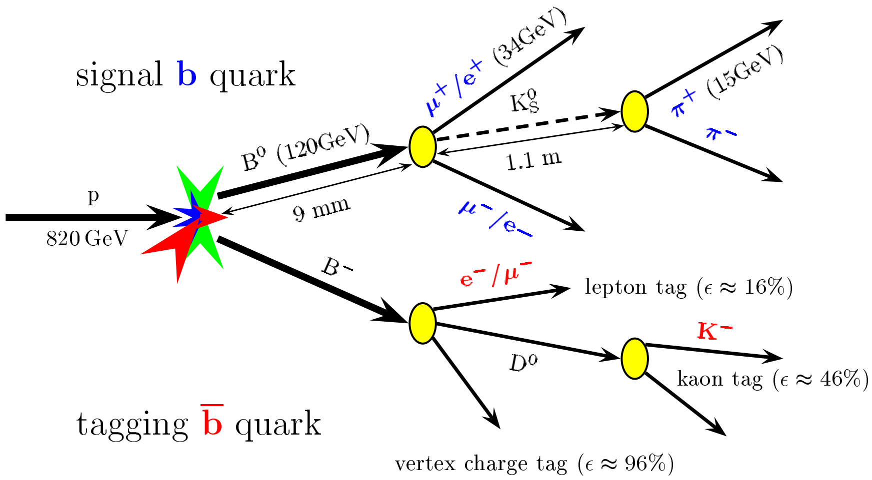

Figure 8.8: The *golden* decay $B^0 \to J/\Psi K_S^0; J/\Psi \to e^+e^-, \mu^+\mu^-; K_S^0 \to \pi^+\pi^-$. The following probabilities apply: 1) production target $\sigma_{B^0\overline{B}^0}/\sigma_{\text{inel}} \approx 8\times10^{-7}$; 2) branching ratio product from decay vertices $5\times10^{-4}\cdot 0.12\cdot 0.69$ 3) trigger, track and vertex reconstruction efficiency 0.17 4) tagging 0.07.

At HERA-B the tails of the coasting 920 GeV proton beam strike an internal wire target producing 10^9 B-mesons per year similar to Fermilab, and about 10 times more than at the B-factories. Since the B-production cross section rises strongly with energy, ultimately, at the 7 TeV pp-collider LHC typically three orders of magnitude in rate can be gained, which is why B-physics plays a central role in the CMS-program, too, as we indicated in previous annual reports. The disavantage of hadronic production is, that only one in 10^6 interaction produces a B-meson pair, i. e. 10^{15} interactions have to occur within the detector to produce 10^9 B-mesons, with 1000 golden decays $B^0 \to J/\Psi K_S^0; J/\Psi \to e^+e^-, \mu^+\mu^-; K_S^0 \to \pi^+\pi^-$ (see Figure 8.8) among them detected. The HERA-B detector (see Figure 8.9) has to be able to select one interesting decay in 10^{12} interactions, withstand an event rate of 40 MHz and a particle density of $10^{-5}R^{-1}/\text{mm}^2\text{s}$, where $R\,[\text{cm}]$ is the perpendicular distance to the beam axis.

At the beginning of 1999 only a fraction of the HERA-B detector was installed yet [4, 5]. One complete station and three half stations of a total of eight of the vertex detector are available. The electromagnetic calorimeter has all tubes installed, the RICH is operating and a major part of the muon system is ready, too. For the outer tracker a revision of construc-

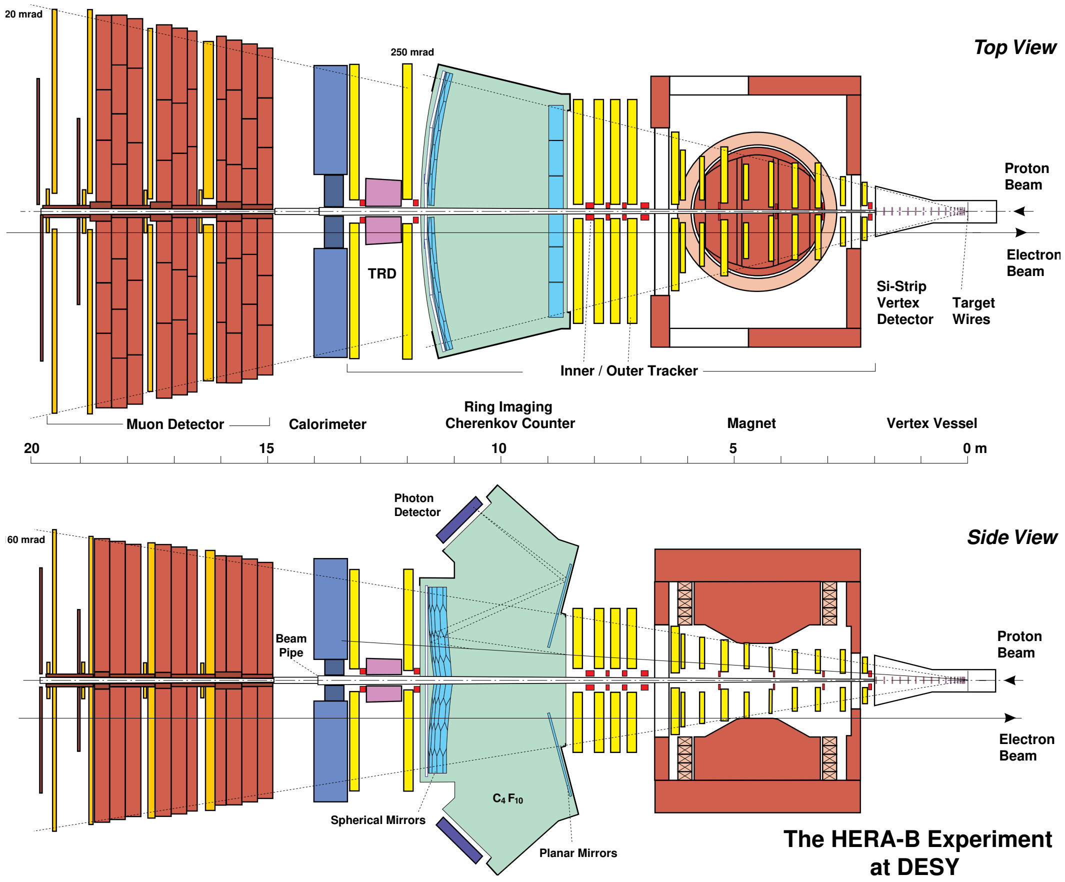

Figure 8.9: The HERA-B detector: magnet bending power 2 Tm; inner tracker ($R < 20$ cm) with MSGC-GEM; outer tracker with 5 and 10 mm drift cells; electromagnetic calorimeter with W/Pb scintillator shaslik; muon system with tube, pad and gas pixel chambers; vertex detector with 12 μm resolution Si strips; ring imaging Čerenkov counter (RICH) with multianode photomultipliers.

tion materials and techniques based on extensive beam tests has led to the start of module production; a small number of modules is being tested within the HERA-B environment. The inner tracker is completely missing for the reasons discussed above. Plans for the short shutdown in May 1999 include the completion of the vertex detector and the muon system, and instal one third of both outer and inner tracker. Whether the latter goal can be reached is doubtful in view of the MSGC ageing problems which are still under investigation. The detector systems which are available at the moment however allow a parallel commissioning of the readout and trigger electronic and data acquisition system. The HELIX chip can in its present version (HELIX2.2) only be used for the silicon vertex detector and not the inner tracker because the trigger outputs fail. The next iteration (HELIX3.0) is presently being tested, but a series will not be ready for the 1999 installation. The readout electronic for RICH, outer tracker and the muon system is completed. The first level trigger is derived so far only from part of the calorimeter, but allowed commissioning of the final DAQ system and calibration of those subsystems, which are operative. It is foreseen to measure the B meson production cross section early this year, and hoped to see the first few example of the J/Ψ decay chain early next year.

The merits of the different CP violation experiments in the B system are usually evaluated by comparing the uncertainty with which the angles of the unitarity triangle (see Figure 8.10) can be measured. If the Wolfenstein parametrisation of the quark-mixing matrix is used as

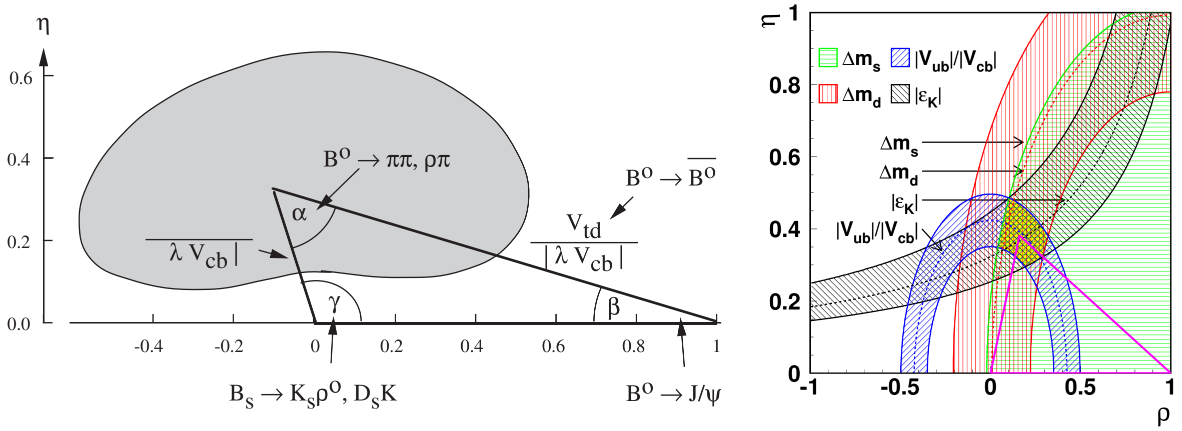

Figure 8.10: The unitarity triangle in the Wolfenstein parametrisation of the Cabbibo-Kobayashi-Maskawa mixing matrix. Left: the different B-meson decay channels which contribute to the determination of the angles and sides of the unitarity triangle to be studied in the HERA-B experiment. The shaded area indicates the uncertainty in the position of the tip of the triangle at the time of the HERA-B proposal. Right: summary of present knowledge on the triangle using K-decay and (indirect) information from LEP experiments [6]

$$\begin{pmatrix} V_{ud} & V_{us} & V_{ub} \\ V_{cd} & V_{cs} & V_{cb} \\ V_{td} & V_{ts} & V_{tb} \end{pmatrix} = \begin{pmatrix} 1-\frac{1}{2}\lambda^2 & \lambda & A\lambda^3(\rho - i\eta) \\ -\lambda & 1-\frac{1}{2}\lambda^2 & A\lambda^2 \\ A\lambda^3(1-\rho-i\eta) & -A\lambda^2 & 1 \end{pmatrix} ,$$

the unitarity triangle is the geometrical representation of the condition

$$V_{ud}V_{ub}^* + V_{cd}V_{cb}^* + V_{td}V_{tb}^* = 0 \ .$$

The complex phase η of the matrix is directly related to CP violation.

The *golden* decay mode is favored, because hadronic uncertainties are small, the CP-asymmetry and the two leptons from J/Ψ decay offer good trigger conditions. If the initial flavor (b or $\overline{b}$ is tagged with the second B meson (see Figure 8.8) the time integrated $B_0\overline{B}_0$ asymmetry affords a measurement of $\sin 2\beta$ with an accuracy of about 0.13 comparable to CDF, and not quite as good as BaBar and Belle. A similar uncertainty can be expected for $\sin 2\alpha$ from $B^0 \to \pi^+\pi^-$, but here the interpretation and experimental conditions are less clearcut.

If the precise measurements of the B_d^0 oscillation frequency, the limit on the B_s^0 oscillation frequency, the improved determination of the mass of the top quark, and of $|V_{ub}|$ are used as input [6] one arrives at the limits shown in Figure 8.10, which correspond to $\sin 2\alpha = 0.06 \pm 0.40$, $\sin 2\beta = 0.75 \pm 0.09$, $\rho = 0.160 \pm 0.085$ and $\eta = 0.381 \pm 0.060$. This analysis, though performed within and consistent with the standard model, rests on the assumption, that the theoretical uncertainties of a number of non-perturbative hadronic quantities, have been properly assessed, which is why it does not make the new generation experiments superfluous.

The HERA-B experiment therefore still very well justified. It may be seen as a prototype and pioneering experiment, from a physics as well as a technology point of view for the considerably more ambitious LHCb and CMS projects in this area.

References

[1] Physik-Institut, Universität Zürich, Annual Report 1997/98, available at *http://www.physik.unizh.ch/jb/1998/kap4.ps*

[2] *Operation of a large GEM-MSGC detector in a high intensity hadronic test beam using fully pipelined readout electronics*, HERA-B int. note 98-149, available at *http://www-hera-b.desy.de/notes/98/98-149.ps*

[3] *First ϵ'/ϵ result from the KTeV experiment*, P. Shawhan, Fermilab (February 1999), available at *http://fnphyx-www.fnal.gov/experiments/ktev/epsprime/epsprime.html*

[4] *The HERA-B experiment*, C. Padilla, 26^{th} Int. Meet. on Fundamental Physics, Illa da Toxa, Pontevedra (Spain) (June 199) available at *ftp://ftp.desy.de/pub/herab/talks/Winter-Meeting/toja.ps*

[5] HERA-B status report, January 1999, R. Eckmann, available at *ftp://ftp.desy.de/pub/herab/talks/prctalk/prc_Jan99.PDF*

[6] *Indirect measurement of the vertex and the angles of the unitarity triangle*, S. Mele, preprint CERN-EP/98-133, (hep-ph/9810333)